ELSEVIER

International Journal of Mass Spectrometry 216 (2002) 131–153

International Journal of Mass Spectrometry

www.elsevier.com/locate/ijms

Review

High-resolution photoelectron-spectroscopy of radicals

Ingo Fischer

Institut für Physikalische Chemie der Universität Würzburg, Am Hubland, D-97074 Würzburg, Germany

Received 25 January 2002; accepted 20 February 2002

Abstract

The occurrence of radicals in various reactive environments and the importance of the ionization energy as a thermochemical property has motivated a large number of experiments on radicals using photoelectron-spectroscopy (PES). In this review we summarize and discuss PES of radicals performed at a resolution of better than 1 meV, with a focus on experiments applying zero kinetic energy (ZEKE)-spectroscopy and other methods based on the pulsed field ionization (PFI) of molecular Rydberg states. The basic physics of PFI, as well as the typical experimental set-up will be described. Subsequently the spectra of selected radicals will be discussed, emphasizing the scientific interest motivating the experiments. Particular attention is given to the methods used to generate the respective radical. (Int J Mass Spectrom 216 (2002) 131–153) © 2002 Elsevier Science B.V. All rights reserved.

Keywords: High-resolution photoelectron-spectroscopy; ZEKE-spectroscopy; Ionization energies; Radicals; Reactive intermediates

1. Introduction

In this paper we review investigations of radicals by high-resolution photoelectron-spectroscopy (PES), with an emphasis on experiments using zero kinetic energy (ZEKE) PES and related techniques that build on the pulsed field ionization (PFI) of Rydberg states. In this context high-resolution means that the low-frequency vibrational structure and, at least for small molecules, the rotational structure of the corresponding ions is resolved, which requires a resolution of better than 1 meV. Since the energy resolution of conventional PES is typically limited to 10–15 meV [1,2], one can only achieve this goal by applying more advanced technology, in particular ZEKE-spectroscopy, which is therefore in the center of this review.

Isolated radicals appear as reactive intermediates in high-energy environments, like combustion engines, hydrocarbon crackers, the atmosphere and interstellar space. Often the chemistry of such systems is dominated by a few key radical species. From the viewpoint of basic research, radicals show rather interesting structural properties, making them model compounds to investigate the dynamics of chemical reactions.

Let us first summarize what sort of information can be gathered from high-resolution photoelectron-spectra:

- PES yields accurate ionization energies (IEs). The IE is one of the most important thermochemical quantities, since binding energies can be extracted through thermochemical cycles [3], as depicted in

[1] E-mail: ingo@phys-chemie.uni-wuerzburg.de

1387-3806/02/$ – see front matter
PII S1387-3806(02)00592-4

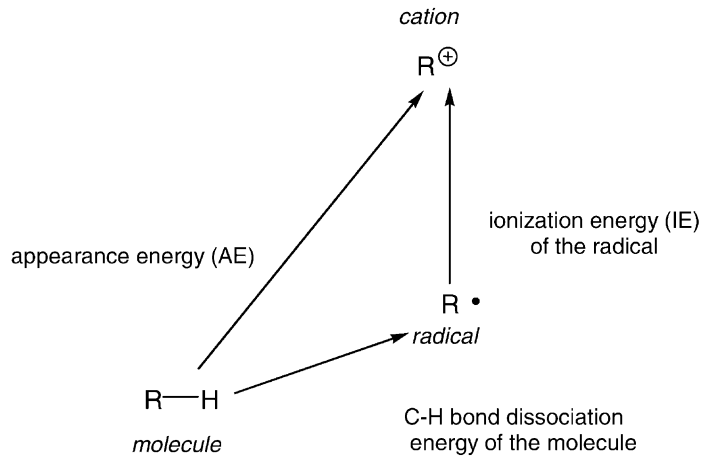

Fig. 1. Bond dissociation energies can be calculated from thermochemical cycles when ionization (IE) and appearance energies (AE) are sufficiently well known. AEs are mostly obtained from mass spectrometry, while accurate IEs are measured by high-resolution photoelectron-spectroscopy.

Fig. 1. The second quantity necessary to complete the cycle, the appearance energy (AE), is typically available from mass spectrometry. However, it was recently demonstrated that accurate AEs can also be obtained from ZEKE-spectroscopy [4], as will be discussed below.

- Detailed structural information is necessary to identify the cations of radicals (which are themselves in most cases closed-shell species!) in high-energy environments, like interstellar space, where radicals are long-lived due to the low collision frequency, but can easily be ionized by the high-energy background radiation, thus becoming important for ion–molecule chemistry.
- In some cases cations of radicals show (or are expected to show) non-classical structures. Well-resolved spectra should permit to extract accurate data on the potential energy surface of such species.
- From high-resolution photoelectron-spectra information not only on the cation but also on the neutral can be deduced. For example, radicals often possess a number of low-lying electronic states that show non-adiabatic couplings. If photoelectron-spectra are recorded by resonant excitation via such intermediate states, the spectra will reveal details on the intermediate state coupling.

Due to the importance of radicals, many of them were investigated already by conventional PES [5,6]. Considerable information can be obtained in particular when the spectra are deconvoluted in a Franck–Condon (FC) analysis [6]. Since some 15 years, however, ZEKE-spectroscopy permits to overcome many of the limitations of PES [7,8], in particular the difficulty of obtaining an accurate energy calibration.

The physics behind ZEKE-spectroscopy, the technology and several applications in molecular spectroscopy have been described in various articles [8–13,141]. In contrast, we will here survey the investigations of open-shell species with a particular focus on results obtained in the last couple of years. Nevertheless we will first summarize the present picture of the mechanism of ZEKE-spectroscopy. This is followed by an introduction of the typical experimental set-up as well as of the various methods for generating radicals. We will then briefly summarize the theoretical and computational approaches to analyze ZEKE-spectra. Finally we will discuss the spectroscopy of a selected number of radical species. We do not include the vast number of conventional PES experiments here, with the exception of a few studies that achieved rotational resolution of small radicals and thus qualify as high-resolution experiments.

Most authors of reviews are selective with respect to the material to be included, the present one being no exception. Thus, two classes of open-shell systems have been deliberately excluded from the review. The first are metal clusters, who are often high-spin systems and might therefore be considered to be radicals as well. In any case they are, like most radicals, reactive intermediates. However, ZEKE-spectroscopy of metal clusters is often driven by motivations different from those in the spectroscopy of molecules. In addition this field was reviewed quite recently [14]. The second class are anions, who are also reactive intermediates, many of them with an unpaired electron. They are excluded because the techniques used to study anions deviate from the way ZEKE is done usually, and because of differences in the physics of the process and in the selection rules. Several articles on various aspects of the photoelectron- and ZEKE-spectroscopy of anions provide the interested reader with more insight [15,16].

2. Pulsed field ionization: the physics behind ZEKE-spectroscopy

The physics underlying ZEKE-spectroscopy was a matter of considerable debate over more than a decade after the introduction of the technique. In the last couple of years, however, a generally accepted picture of the mechanism has emerged [17,18]. Originally ZEKE was thought to be a new variant of threshold photoelectron-spectroscopy (TPES) [19,20]. In TPES a time-of-flight electron analyzer is fixed at zero kinetic energy and the light source tuned over the ionization threshold. Thus, a signal appears only when the photon energy is exactly in resonance with an eigenstate of the ion. The new idea, introduced in 1984, was to use a field-free delay time before the electrons are extracted from the ionization region by a pulsed dc field [7]. During this delay time on the order of 1 μs all kinetic electrons leave the interaction region. The electrons with zero kinetic energy were assumed to stay behind and to be accelerated by the pulsed field towards the detector. The use of pulsed extraction fields led immediately to an increase of resolution by two orders of magnitude as compared to conventional PES.

In the late 1980s it was demonstrated that ZEKE-spectroscopy does not rely on the detection of free electrons, but rather on the PFI of high-n Rydberg states, a few cm^{-1} below the ionization threshold [21]. For this reason the technique is sometimes referred to as PFI or PFI-PES. Since in these high-n states the electron is far away from the core, it has a no influence on its structure, which is therefore identical to the cation. Due to accidental stray fields present in most apparatuses all kinetic electrons, including those with zero kinetic energy are removed from the interaction region during the delay time. However, the fact that optically prepared high-n low-l Rydberg states are long-lived was rather surprising, since back-of-the envelope calculations showed that molecular Rydberg states should decay by predissociation or autoionization in significantly less than 1 μs [22,23]. After several years of controversial experiments and stimulating discussions a consistent picture has been developed [17]. There is a general agreement that the unexpectedly high stability of the Rydberg states is due to (a) stray fields present in most of the experiments [22–25] and (b) interactions between Rydberg states and nearby ions [26–29], i.e., time-varying electric fields. The former leads to a mixing of the l, the latter to a mixing of the m_l quantum number, and thus to the formation of Rydberg states with high-n, -l, and -m_l. These states do not decay on the time scale of the experiment, because of a low probability for core-electron interactions leading to autoionization or predissociation. Expressed in a more formal language, l and m_l are not good quantum numbers in the presence of electric fields. However, the eigenstates can always be expressed as a superposition of l and m_l states, with a large contribution originating from states with high l and m_l quantum numbers. The mixing leads to an increase in lifetime by a factor of roughly n^2.

The situation is summarized in Fig. 2, which describes a Rydberg series converging onto the rotational ground state of the cation, $N^+ = 0$. The highest-lying Rydberg states in a narrow region roughly 1–2 cm^{-1}

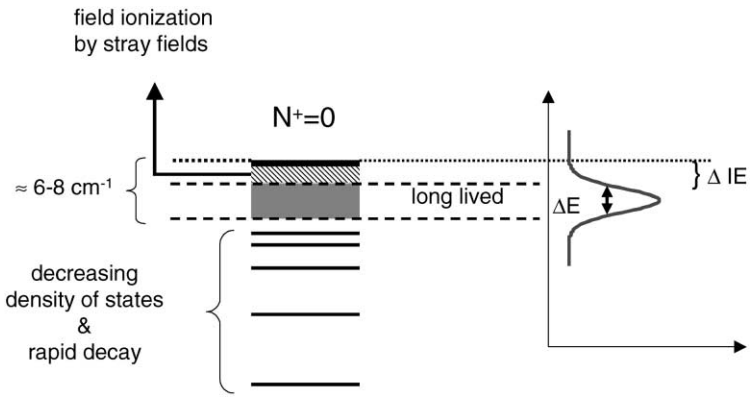

Fig. 2. The highest-lying Rydberg states, 1–2 cm^{-1} below the ionization threshold, are often ionized by stray fields during the delay time. The next group of states, down to 6–8 cm^{-1} below the threshold contribute to the ZEKE-signal. Below this region the density of Rydberg states decreases and the probability of decay during the delay time increases rapidly. The width of the signals, ΔE, depends on the magnitude of the extraction field and on the laser bandwidth. The measured ionization energy is shifted by ΔIE relative to the true IE.

below the ionization limit are ionized by stray fields and removed during the delay time; thus they do not contribute to the signal. This leads to a slight red-shift of the measured ionization energy. The next group of states, comprising a range of approximately 6 cm^{-1}, become long-lived due to l and m_l mixing. These states are ionized by PFI and contribute to the signal. They constitute the detection window. The width of the ZEKE peak, ΔE, and thus the spectral resolution are determined by the magnitude of the extraction field; very small pulsed fields ionize only a small region of Rydberg states, resulting in a small ΔE. The difference between the onset of the ZEKE peak and the true ionization threshold yields ΔIE, the error in the ionization energy.

Although the peak width ΔE is proportional to $F^{1/2}$, the square root of the extraction field, over a certain range, it does not become larger than 6–8 cm^{-1}, even with large extraction fields, provided that a narrow-bandwidth laser is used. First, Rydberg states below this energy range decay faster, and second the density of states, scaling with n^3, diminishes rapidly. Rydberg states with $n \ll 150$ thus do not contribute significantly to the signal. Thus, the roughly 6–8 cm^{-1} broad region below the ionization threshold, with n ranging roughly from 150 to 300 that gives rise to the ZEKE signal is sometimes referred to as the "magic region."

It is also evident that the best spectral resolution and the most accurate IEs are obtained when the region of field ionized Rydberg states becomes as small as possible. To achieve this goal Müller-Dethlefs and coworkers used multistep staircase extraction fields [30,31], while Merkt and coworkers reduced stray fields as much as possible and applied very small extraction fields [32,33] in order to obtain high-resolution and accurate IEs. When the experiments are carried out this way, the spectral resolution is at present limited by the bandwidth of the light source (0.1–0.2 cm^{-1}). However, the resolution can only be optimized at the cost of signal size, because the largest signals are obtained when the whole "magic region" is field ionized and detected at once. Since in investigations of radicals the experimentalist is often starving for signal, spectra are generally recorded at a somewhat lower resolution between 1 and 6 cm^{-1}, or roughly 0.1–1 meV.

3. The experimental set-up

Experiments on radicals are best performed in molecular beams in order to isolate the radical from its environment and to suppress bimolecular reactions. Since ZEKE is an inherently pulsed technique, pulsed beams are used in the majority of experiments.

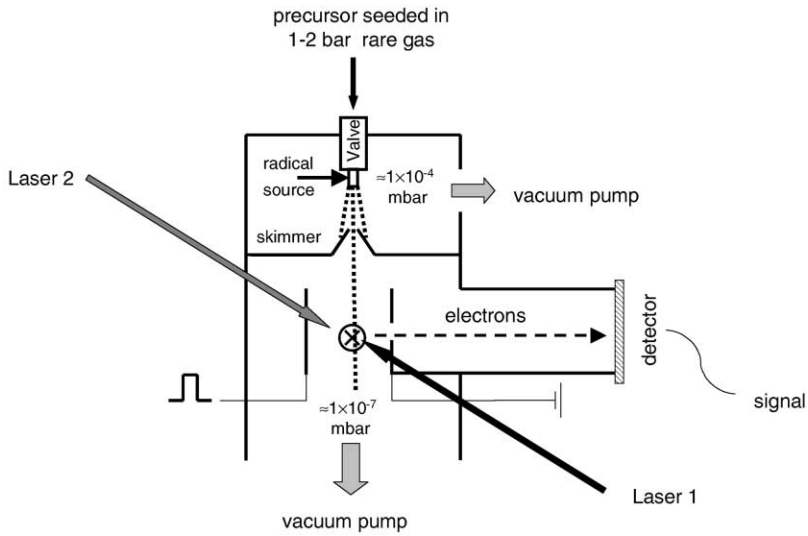

Fig. 3. ZEKE experiments are typically performed in pulsed molecular beam machines. Laser excitation occurs under field-free conditions in the interaction region of a simple time-of-flight mass spectrometer. After a field-free delay time of roughly 1 μs, during which all kinetic electrons escape from the interaction region, a pulsed electric field is applied, field ionizing the high-lying Rydberg states populated by the laser and accelerating the electrons towards the detector.

A typical set-up for ZEKE-spectroscopy is depicted in Fig. 3. A precursor, diluted in 1–2 bar of a rare gas, is expanded through a pulsed valve into the vacuum. Typically one of the radical sources discussed below is attached to the faceplate of the valve. In the subsequent adiabatic expansion the radicals formed in the source are internally cooled by collisions with the carrier gas atoms and then enter the collision-free regime where the radicals are frozen and no further interactions occur [34].

After passing through a skimmer the beam enters the second chamber, where the spectroscopic experiment is performed. In the ionization region the molecular beam is crossed by one or two laser beams for excitation and ionization. After a delay time of around 1 μs a negative pulse (typically, but not necessarily, between 1 and 10 V/cm) is applied to one of the electrodes. The Rydberg states are field ionized and all electrons are accelerated towards a detector. The electron signal is recorded as a function of laser wavelength.

Often rather simple time-of-flight mass spectrometers are used for electron detection. One has to be aware, though, that electrons are sensitive to the magnetic field of the earth, thus proper magnetic shielding has to be used. On the other hand, several groups demonstrated excellent spectral resolution with very short flight tubes of a few centimeter length [35,36]. In this case magnetic shielding is superfluous. Alternatively other devices for electron detection, like magnetic bottles [37–40], are sometimes employed in ZEKE-spectroscopy.

Beside ZEKE-spectroscopy several related techniques exist that rely on the PFI of Rydberg states, the most important being mass analyzed threshold ionization (MATI) [41–44]. Here the corresponding ions are detected instead of the electrons, yielding mass information in addition to the spectroscopic information, clearly a big advantage when reactive molecules are studied that can only with difficulties be generated cleanly. The underlying physics is the same as for ZEKE. In fact, often the term PFI spectroscopy is used for both, and several other related, methods in order to emphasize the similar mechanism. We prefer to use the acronyms ZEKE or MATI to make clear whether electrons or ions are detected.

MATI also has some disadvantages as compared to ZEKE. Due to the higher masses of ions as compared to electrons the difference in velocity between prompt ions and ions originating from field ionization is rather small. The separation between the two, straightforward in ZEKE, where you just have to wait long enough, requires a sequence of pulses and offset fields in MATI. In addition the signals obtained upon MATI are smaller than those obtained by ZEKE, because due to the larger offset fields a larger range of Rydberg states is field ionized during the wait time (see Fig. 2). Therefore, only two radicals have been studied by MATI, CD_3 and ND_4, which will both be discussed below. The spectral resolution achievable in MATI is in principle similar to ZEKE [44], but in practice often inferior due to experimental difficulties.

4. The generation of radicals

Spectroscopy on radicals poses significant challenges to the experimentalist. It is still difficult to generate radicals cleanly and in a high enough number density to perform spectroscopic experiments. In addition it is often unavoidable to generate, beside the species of interest, a second fragment from the precursor that can in principle interfere in the spectrum. Typically a chemical bond in a suitable precursor is cleaved by means of pyrolysis, photolysis or electric discharges. Modern experiments are generally performed in supersonic beams in order to avoid reactive collisions. Since ZEKE is an inherently pulsed technique, it is ideally combined with pulsed radical sources and pulsed molecular beams.

Pyrolysis is a rather old technique and is quite commonly applied in conventional PES (see [6] for a summary). In earlier experiments vapor at low pressure was passing under effusive flow conditions through a heated tube coupled directly to the ionization region of the spectrometer. Under these conditions secondary reactions, leading to the destruction of the radicals and/or the formation of unwanted side products, were unavoidable. The problems are largely solved in a high pressure flash pyrolysis source coupled with a supersonic expansion, introduced in the mid-1980s [45,46]. In this design, depicted in the left-hand trace of Fig. 4, an electrically heated silicon carbide tube with a length of 10–20 mm and a diameter of 1 mm is mounted onto a molecular beam source with an orifice of 0.6–0.8 mm. A suitable precursor, diluted in 1–2 bar of a rare gas is expanded through this nozzle into the vacuum. Under these conditions a fast flow velocity of the gas is achieved, which leads to short contact times with the heated wall on the order of some 10 μs and correspondingly few secondary reactions. A variety of radicals and carbenes has been generated by this method in high number density [3,6,47]. Flash pyrolysis sources have been successfully combined

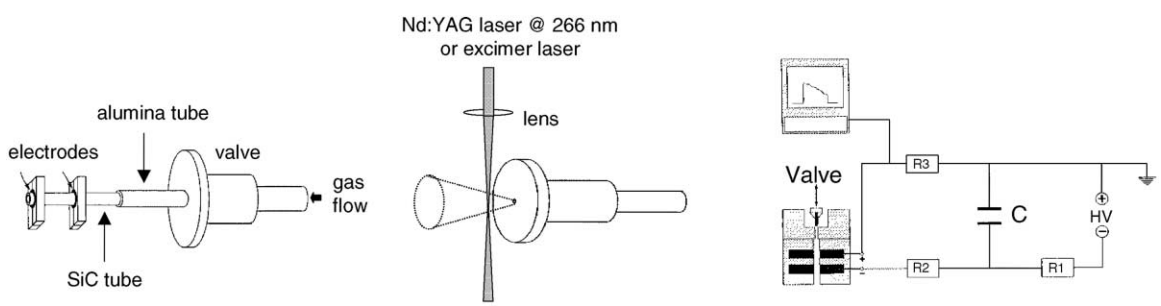

Fig. 4. Various radical sources can be coupled to pulsed molecular beams. In flash pyrolysis (left-hand trace) the precursor flows through an electrically heated SiC tube. During the residence time of around 10 μs enough energy is deposited in the molecule to cleave the thermally most labile bond. In photolysis (center trace) the precursor molecule is excited into a directly dissociative state by laser excitation. In an electric discharge source (right-hand trace) the flow of the precursor gas closes the circuit, leading to a discharge that causes fragmentation of the precursor and generation of the radical. In all three sources the radicals are cooled in the subsequent supersonic expansion.

with a variety of other spectroscopic techniques over the last couple of years, like microwave spectroscopy [48] or translational energy spectroscopy [49].

The selectivity of the method is demonstrated in Fig. 5, using the generation of the propargyl radical, C_3H_3, by flash pyrolysis of propargyl bromide as an example. Photoionization mass spectra recorded with 121.6 nm VUV light were obtained with the pyrolysis source off (upper trace) and on (lower trace). As visible, the precursor is almost quantitatively converted and no side products are visible. A radical density of more than 10^{14} cm^{-3} is achieved at the exit of the pyrolysis source.

Photolysis is probably the most common method for the generation of radicals. It relies on the laser excitation of the precursor molecule to an electronic state that dissociates directly into the radical of interest plus a second fragment. Especially for organic radicals iodides are often used as precursors because they generally have dissociative states in the UV that can conveniently be excited with the fourth harmonic

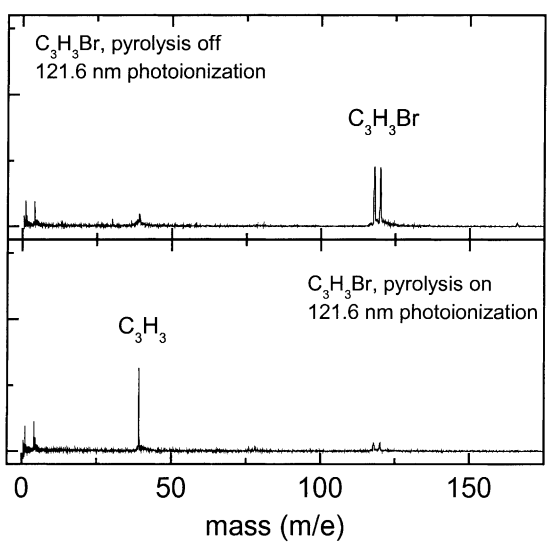

Fig. 5. Photoionization mass spectra ($\lambda_{ion} = 121.6$ nm) illustrating the generation of propargyl, C_3H_3, by flash pyrolysis of C_3H_3Br. With the pyrolysis source off (upper trace), only little fragmentation of the precursor is evident. When the pyrolysis source is turned on (lower trace), a signal due to propargyl appears, whereas the precursor signal disappears almost completely.

of a Nd:YAG laser at 266 nm or a 248 nm excimer laser. Photolysis can easily be coupled to supersonic beams by focusing the laser a few mm behind the pulsed valve orifice, as depicted in the center trace of Fig. 4. The radicals will then be internally cooled in the subsequent expansion. Alternatively the photolysis is often performed in the ionization region itself and can then also be coupled with an effusive source. In this case hot radicals with a significant amount of internal energy are probed in the subsequent spectroscopic experiment. While this is tolerable in experiments on small radicals where rotational resolution is obtained, it might lead to spectral congestion and assignment ambiguities in investigations of larger radicals. Sometimes the same tunable laser system used to record the ZEKE-spectra is also used to photolyze the precursor in the first place. In this case the band intensities in the spectrum depend not only on the absorption cross-section of the radical, but also on the cross-section of the precursor.

The general disadvantage of photolysis is the need for a laser as the light source in order to obtain a high enough photon flux for efficient radical generation. This makes the technique more expensive than pyrolysis, but also more difficult due to the need for accurate temporal synchronization between photolysis- and spectroscopy-laser. It is also conventional wisdom that the duty cycle of an experiment scales with the square of the number of lasers involved. In addition one photolysis-laser is not enough to set-up a general radical source. Although many radicals have good precursors dissociating upon 266 nm excitation, many other, in particular inorganic radicals are not accessible at this wavelength, and require, e.g., 193 nm excimer radiation. Thus, a tunable system is required for a general photolysis source. Nevertheless many radicals, in particular oxygen-containing species, have been successfully generated by photolysis [50,51].

Electrical discharges are also commonly utilized to generate radicals. They are easily coupled to supersonic jet sources [52], and radical yields are often quite good. A typical set-up for a pulsed electric discharge [53,54] is depicted in the right-hand trace of

Fig. 4. An insulating teflon block with a small channel, containing two electrodes, is mounted onto the pulsed valve. When the valve opens, and the molecules pass through the channel, the circuit is closed and bonds in the precursor are cleaved in the occurring discharge. Similar designs have been reported by other groups as well [55]. Discharge sources often suffer from a lack of selectivity, with many side products being present. Thus, they are the source of choice if one is interested in thermochemically unfavorable radicals, that are often not available by any other technique. Nevertheless recent IR laser diode studies successfully employed discharge sources [56] to generate allyl [57] and ethyl [58] in high number densities of more than 10^{14} cm^{-3}. The authors also claim clean generation with little or no side products. Due to the MHz resolution, spectral congestion is avoided in these experiments and the rotationally resolved bands can be unambiguously assigned to a particular species. Discharge sources have been employed in conventional PES, but to the authors best knowledge no ZEKE-spectra have yet been reported employing them.

Many other techniques for the generation of radicals have been reported. For example, laser vaporization of metal rods is the method of choice for producing metal clusters or metal-containing molecules [59,60]. Dyke and coworkers used another interesting approach, abstraction of hydrogen from closed-shell molecules by fluorine atoms in a flow reactor, to produce radicals for PES [5]. This source, like many others, works well under effusive conditions, but is not easily combined with supersonic pulsed beams. There is only one example of a radical studied by ZEKE-spectroscopy that was generated in a continuous source, the OH radical, which will be discussed below.

4.1. Excitation schemes

There are three techniques to optically excite molecules into high-lying Rydberg states, depicted in Fig. 6: (1) one-photon VUV excitation (center), (2) resonant (left-hand side) and (3) non-resonant (right-hand side) multiphoton excitation. All three

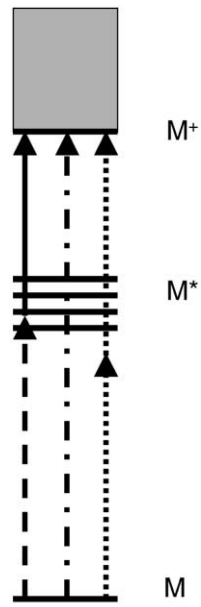

Fig. 6. Three different schemes are used to excite the molecules into a high-*n* Rydberg state. In experiments on stable molecules resonant two- or multiphoton excitation with two different laser colors (dashed and full arrow) via selected intermediate states is commonly used, simplifying the ZEKE-spectra. For radicals the more general one-photon excitation scheme (dash-dot arrow) is often preferential, because intermediate electronic states are either unstable or not well characterized. In several experiments non-resonant multiphoton excitation schemes (dotted arrows) have been successfully applied.

of them have been applied to study radicals by ZEKE-spectroscopy.

In most ZEKE experiments, spectra are recorded by resonant multiphoton excitation (REMPI). A first laser, fixed at a resonant excitation frequency, populates a selected intermediate vibronic or rovibronic state, a second tunable laser subsequently promotes the molecule into a high-lying, long-lived Rydberg state. This scheme has two advantages: first, intermediate state selection reduces the number of lines and thus the complexity of the spectrum; second, by recording ZEKE-spectra through different intermediate states a larger part of the ionic potential energy surface can be explored. This scheme, successfully applied to many stable molecules and diatomic radicals, does unfortunately not work for most polyatomic radicals, because

often the excited electronic states are short-lived, or simply not well characterized. One-photon excitation by tunable VUV radiation is thus a more general approach [61,62]. Due to the low ionization energy of most polyatomic radicals, difference frequency mixing in a gas cell is the method of choice for recording rotationally resolved ZEKE-spectra. However, it is still difficult to produce VUV radiation on a laboratory scale that is tunable over a large enough range to sample a number of vibrational states. Alternatively synchrotron light sources provide VUV and XUV light tunable over a wide range for ZEKE-spectroscopy [63,64]. One has to deal though with the challenges associated with carrying out experiments at large scale facilities. The third excitation scheme is non-resonant two- or multiphoton excitation from the neutral ground state [65]. Since only one tunable laser is required the scheme is particularly simple. However, modulation of the spectra by accidental intermediate resonances [66] and competing processes of higher photon order might interfere in the experiments. Despite these disadvantages ZEKE-spectra of several closed-shell molecules and radicals have been obtained this way.

4.2. Theory and computation of ZEKE-spectra

Since all molecular properties are continuous at the ionization threshold, two different approaches can be used to interpret the spectra. One comes from "above," i.e., from higher energies, considering the ZEKE electrons as very low energy photoelectrons, the other one comes from "below," i.e., from lower energies, and discusses ZEKE-spectra as optical spectra with transitions terminating in a final state with pure Hund's case (d) angular momentum coupling. Both approaches yield in principle the right answer.

Rotational selection rules, based on angular momentum conservation, are relaxed relative to usual bound–bound spectroscopy, because in addition to the rotational quantum number of the initial and the final state the angular momentum of the electron has to be taken into account. Thus, transitions with ΔN or $\Delta K > 1$ are observed, due to the angular momentum ℓ carried away by the outgoing electron. In a ZEKE-spectrum of a diatomic molecule one thus obtains [67]

$$\Delta J_{\max} = \ell + \tfrac{3}{2} \quad (1)$$

In an atomic-like picture of photoionization [68] a p-electron ($l = 1$) is ejected into the d- or s-continuum ($\ell = 2, 0$), or in terms of bound–bound spectroscopy, excited into high-lying s- or d-Rydberg series. Thus, from the maximum change in angular momentum observed in the spectrum one can gather information on properties of the ejected electron. Note that from a spectroscopic point of view the experiment is over, once the electron is excited to the high-n state. The subsequent processes, including l- and m_l-mixing, as well as the PFI, have to be considered as parts of the detection scheme and do not influence the spectroscopy.

Of course parity conservation holds strictly. When the initial (neutral) and the final (ionic) state are described by pure Hund's case (b) coupling parity conservation can be expressed as

$$\Delta N + \ell = \text{odd} \quad (2)$$

In an atomic picture of photoionization, a p-electron with odd parity is ejected into s- or d-continuum channels with even parity, thus transitions with $\Delta N = \text{odd}$ are expected to dominate the spectrum. Although an electron in a molecule generally has to be described by a distribution of l-values, such a simplified description is in many cases at least qualitatively appropriate.

In symmetric and asymmetric rotors the selection rules for ΔK, or ΔK_a and ΔK_c, respectively, are correspondingly relaxed. The selection rules for symmetric rotors become $\Delta K = \text{even}$ instead of $\Delta K = 0$ for parallel transitions, and $\Delta K = \text{odd}$ instead of $\Delta K = \pm 1$ for perpendicular transitions in ZEKE and PES. For a more extensive discussion of symmetry selection rules underlying ZEKE-spectroscopy, we refer to [69,70].

Vibrational selection rules on the other hand are still a matter of debate. The vibrational structure of photoelectron-spectra should be governed by the FC principle, with only totally symmetric vibrations appearing. In numerous cases, however, significant deviations have been observed [71], in some cases

even a complete breakdown of the FC picture [72,73]. Thus, non-totally symmetric vibrations do appear in ZEKE-spectra and intensity patterns are observed that cannot always be explained within a simple FC-framework. On the other hand, the ZEKE-spectra of many molecules can readily be explained in the FC picture. We will discuss this subject below with special reference to radicals.

For a detailed description of the ionization dynamics two different approaches are applied, multichannel quantum defect theory (MQDT) and ab initio methods, the former corresponding to an approach from "below," the latter to an approach from "above." Quantum defect theory (QDT) relies on the concept of a highly excited electron moving in the Coulomb potential of the ion core [74]. The small probability of finding the electron in the core region leads to non-coulombic components that are responsible for processes like predissociation and autoionization, treated separately as short range interactions. In MQDT [75] the photoabsorption is regarded as the scattering of an electron off the core into independent channels, each channel corresponding to one Rydberg series. The short range interactions are described by a scattering matrix that contains the quantum defects, describing the deviation of a Rydberg state from Coulombic behavior. The basic physical picture of MQDT is well suited for a calculation of ZEKE-spectra. Since it explicitly calculates interactions between the various channels (i.e., Rydberg series), it can account for the irregularities in the intensities due to Rydberg state coupling that are observed in some ZEKE-spectra. However, it requires that the quantum defects are known from experiment or calculation, or that at least a good guess is available. For anything larger than a diatomic this is still a tedious task.

The ab initio method was originally developed to calculate conventional photoelectron-spectra at rotational resolution. It relies on the calculation of transition matrix elements between a bound state and the product of an ionic state and a free electron wave function [76,77]. The ab initio approach from "above" does not take final state interactions due to coupling of Rydberg states into account, and occasionally failed to predict accurate intensities in ZEKE-spectra. On the other hand an impressive accuracy was obtained in calculations of the photoelectron- and ZEKE-spectra of various polyatomic molecules that are still out of reach of a detailed MQDT analysis.

4.3. Discussion of selected radicals

In the following sections high-resolution photoelectron-spectra of several radicals will be discussed. Of course the selection, as well as the depth of the discussion is a matter of personal choice. As mentioned, metal clusters [14] and metal oxides [78] are not considered. On the other hand, we will discuss several complexes of metal atoms with organic radicals. The IEs of all species discussed in this review are listed in Table 1. However, it is not our intention to summarize all available spectroscopic constants. Instead we will focus on the chemical and physical relevance, i.e., describe what makes a given radical

Table 1
Ionization energies of radicals obtained by ZEKE-spectroscopy or high-resolution conventional photoelectron-spectroscopy[a]

Radical	Ionization energy (cm^{-1})	Reference
NO	74721.7	[21]
NO_2	77316	[83]
OH	104989	[84]
OD	105085	[84]
NH	108692	[93]
SH	84057 ($SH^+X^3\Sigma^{-1}$)	[87]
SH	93925 ($SH^+a^1\Delta$)	[40]
ND_4	37490.7	[97]
C_6H_5–CH_2 (benzyl)	58468	[106]
C_6H_5–CD_2	58418	[106]
C_6D_5–CD_2	58386	[106]
CH_3	79349	[99]
CD_3	79287	[100]
C_3H_3	69953	[36]
C_3H_5	65762	[125]
CH_3S	74726	[130]
Mg–CH_3	53265	[101]
Zn–CH_3	58661	[101]
Cd–CH_3	57105	[102]
Zn–C_2H_5	56384	[103]

[a] Metal clusters and metal oxides have been excluded, but some complexes of metal atoms with organic radicals are listed.

so interesting. We will also discuss experimental aspects, in particular the method of generation of the radical, because this is the most interesting aspect for people who want to enter this field.

4.4. Inorganic radicals

In the present context we consider all radicals that do not contain any carbon atoms as inorganic. Most of them are small diatomics with doublet electronic ground states, permitting the comparison with accurate calculations. In addition a few experiments on larger radicals exist.

4.4.1. NO and NO_2

NO and NO_2 served as model cases for open-shell systems for a long time. However, since both molecules are commercially available in bottles, the usual challenge in radical spectroscopy, the clean generation, does not exist. Thus, despite being radicals both molecules cannot be considered to be reactive intermediates in the true meaning of the word. NO was the first molecule to be investigated by ZEKE-spectroscopy [7,21,79], so a vast amount of experiments were carried out over the last 15 years. In the lower trace of Fig. 7, the ZEKE-spectrum of the $X^{+2}\Sigma^{+}$ cationic ground state of NO is shown, obtained by non-resonant two-photon ionization [80] from the $^2\Pi_{1/2}$ electronic ground state, which nicely illustrates several characteristics of ZEKE-spectroscopy. A simulated spectrum is shown in the upper trace, assuming a rotational temperature of 2.5 K. Due to the low temperature that can usually not be obtained when the radicals have to be generated by any of the sources described above, only transitions originating from the two lowest rotational levels, $J'' = 1/2$ and $J'' = 3/2$ are observed. The appearance of transitions into ionic rotational states up to $N^+ = 4$ illustrates the more relaxed angular momentum selection rules in PES. The expected maximum change in angular momentum, ΔJ_{max}, is $\Delta J_{max} = \ell + 3/2$ [67,69,70]. As the unpaired electron in the $^2\Pi_{1/2}$ electronic ground state of NO was calculated to be an electron predominately of d-character [76], which can be ejected into the ℓ = s-, d- or g-continuum, a ΔJ_{max} of 11/2 is calculated. While the maximum change observed in the spectrum in Fig. 7 is $\Delta J_{max} = 7/2$, weak $\Delta J_{max} = 9/2$ transitions were observed for higher J'' states, only populated in somewhat warmer spectra [80]. One can thus conclude that the electron is predominately ejected into the s- and d-continuum channels. Since each rotational level

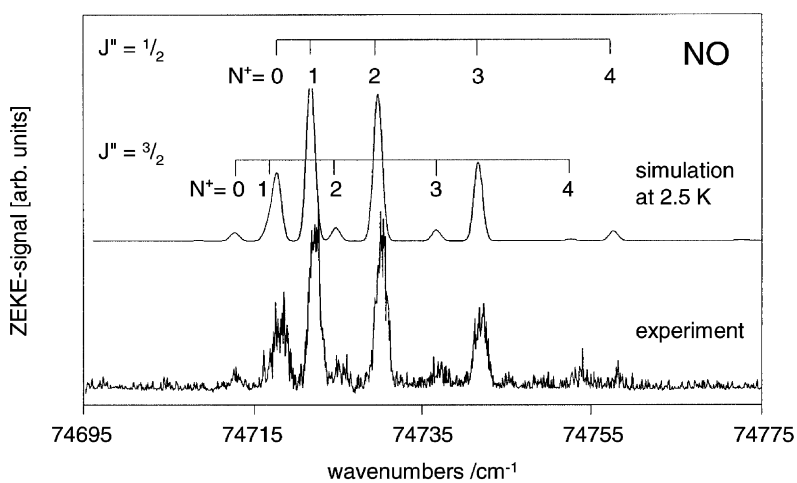

Fig. 7. The ZEKE spectrum of NO, recorded by non-resonant two-photon excitation from the electronic ground state with a simulation assuming a rotational temperature of 2.5 K given for comparison. A change in angular momentum of up to $\Delta J = 7/2$ is apparent.

in NO is split into *e*/*f* sublevels with opposite parity that were not resolved in the experiments, parity is automatically conserved.

ZEKE-spectra of NO_2 [81–83] have also been reported. The focus in this work was an investigation of coupling phenomena between Rydberg series converging onto different vibrational states of the ion.

4.4.2. OH and OD

The OH radical is ubiquitous in many reactive environments, ranging from combustion engines to the atmosphere and interstellar space. Thus, OH and OD were among the first species to be investigated by ZEKE-spectroscopy. Due to the large rotational constants it is straightforward to accomplish rotational resolution. The OH radical is the only species discussed in this paper that was not produced in a pulsed source, but rather in a continuous fashion. It was generated in a flow discharge source through a rapid reaction of H atoms with NO_2, according to

$$H + NO_2 \rightarrow OH + NO$$

The hydrogen atoms were produced in a flowing microwave discharge from a mixture of H_2 and He. The ZEKE-spectra of the $v^+ = 0$ band of OH^+ and OD^+ radical were obtained by one-photon ionization using coherent VUV radiation [84]. In experiments using conventional PES the OH radical has been generated by photolysis of H_2O_2 at 248 nm and formic acid at 222 nm [85,86].

4.4.3. SH

The SH radical was produced photolytically from H_2S by exciting the precursor into the directly dissociative A^1B_1 state. ZEKE-spectra of the $X^{+3}\Sigma^-$ ionic ground state were recorded using a non-resonant two-photon scheme [87]. Here the same laser served as source for photolysis of H_2S in the ionization region, and for ZEKE-spectroscopy. Since the SH radicals were not cooled in a supersonic expansion and no intermediate state was selected, a large number of rotational transitions were observed and not all of them could be assigned unambiguously.

As a comparison, a second experiment on SH, aimed at an investigation of the excited $a^{+1}\Delta$ states of SH^+ and SD^+, shows the power of intermediate state selection [40]. The radicals were also produced in the ionization region and are thus internally hot. In a first step, however, they were excited to various rotational levels of the intermediate $^2\Phi$ Rydberg state. Since the electronic structure of this state corresponds to an $a^{+1}\Delta$ core with an additional 3dπ Rydberg electron, the cross-section to the excited state of the cation, 9867 cm^{-1} above the ionic ground state is very high. To the best of our knowledge this is the only ZEKE investigation of a radical aimed at an excited electronic state of the cation. Individual rotational states of the cationic $a^{+1}\Delta$ state were resolved. The spectra, given in Fig. 8, demonstrate a typical property of many ZEKE-spectra. It is often observed that rotational transitions associated with a decrease in angular momentum, $-\Delta N$ appear with higher intensities than the corresponding $+\Delta N$ transitions. In the spectrum

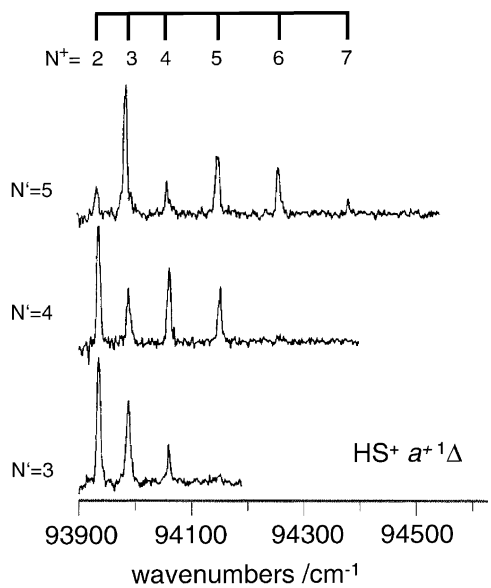

Fig. 8. ZEKE-PFI spectra of the $a^{+1}\Delta$ state of SH^+, obtained by $[2+1']$ excitation via various rotational levels N′ of the $[a^1\Delta]3d\pi\ ^2\Phi$ state. The spectra show an intensity asymmetry: transitions associated with a decrease in angular momentum appear with a higher intensity than transitions associated with an increase (reproduced with permission from [40]).

originating from $N' = 3$ (bottom trace) the $\Delta N = -1$ transition into the $N^+ = 2$ state is considerably more intense than the $\Delta N = +1$ transition into the $N^+ = 4$ state. In the spectra originating from $N' = 4$ and 5 the $\Delta N = -2$ transition represents the most intense peak in the spectrum, while the peaks corresponding to $\Delta N = +2$ are only barely recognizable. This effect is often explained by a coupling of Rydberg states converging to different states in the ion [18,88,89]. In the excitation step one populates in addition to the high-*n* Rydberg states converging to the $N^+ = N - 2$ rotational state of the ion also low-*n* Rydberg states converging to higher N^+ states of the ion. These low-*n* states can couple to the continuum of high-*n* states and contribute additional intensity to the transitions associated with a decrease of angular momentum. In the case of SH, however, the intensity assymetry was also observed in conventional photoelectron spectra, where such couplings are not present. For a complete discussion of additional factors relevant in the spectra of SH I refer to Ref. [86].

4.4.4. Conventional photoelectron-spectra of small radicals

de Lange and coworkers demonstrated that a spectral resolution of less than 10 cm^{-1} can be obtained in a magnetic bottle time-of-flight photoelectron spectrometer under optimized conditions, sufficient to resolve rotationally excited states in the cation [90]. Therefore, for some diatomic radicals rotationally resolved spectra of the ionic ground state were obtained by conventional PES rather than ZEKE-spectroscopy [86], examples being OH [85], SH [91,92] and NH [93,94]. Due to the comparable accuracy, the measured IEs have been included in Table 1. In addition vibrationally resolved spectra have been obtained for the ClO radical [95]. Since the only constraint on the energy of the laser is that it has to be sufficient to ionize the molecule, the spectra can be recorded through selected intermediate states with one laser only. The advantage of a magnetic bottle is its high collection efficiency of around 30–50%. Thus, for conventional PES of reactive intermediates, which can only be produced in small number densities, it is superior to conventional time-of-flight analyzers.

Typically the radicals were generated photolytically in the ionization region of the spectrometer, leading to vibrationally and rotationally hot radicals. In this type of experiment this is not necessarily a disadvantage: first, it is much easier to achieve rotational resolution for high-*J* states, and second, spectral congestion is avoided by intermediate state selection. Since each spectrum is obtained at a fixed frequency, the relative peak intensities are independent on the absorption cross-section of the precursor.

As an example, we will discuss the rotationally resolved spectrum of the NH cation [93], given in Fig. 9. Formally NH, termed imidogen, with its $X^3\Sigma^-$ ground state is not a radical, but should rather be regarded as the simplest nitrene. It has been produced by photolysis from HN_3, yielding electronically excited NH in its a $^1\Delta$ state. The experimental spectrum obtained by [2 + 1] REMPI through the $f^1\Pi(3p\sigma)$ $v' = 0$, $N' = 13$ Rydberg state is given on the left-hand side of Fig. 9. Transitions into the $v^+ = 1$ state are small compared to transitions into the $v^+ = 0$ state, due to the similar geometry of intermediate state and cation. Interestingly the spectrum is dominated by even ΔN

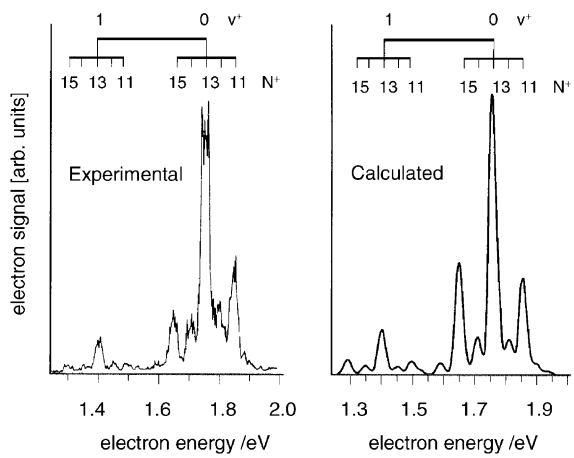

Fig. 9. Experimental (left-hand trace) and ab initio calculated (right-hand trace) conventional photoelectron-spectra of NH. The spectrum was recorded through the $f^1\Pi$ ($v' = 1$, $N' = 13$) intermediate state (reproduced with permission from [94]).

transitions ($\Delta N = 0, \pm 2$), although ionization of a p-electron should be associated with odd ΔN transitions due to parity conservation.

An important aspect of rotationally resolved conventional photoelectron-spectra is the possibility for a direct comparison with ab initio calculations that take the wave function of the ejected electron into account. A calculated spectrum is given for comparison on the right-hand side of Fig. 9. As visible, the agreement between theory and experiment is rather convincing. The calculations [94,96] demonstrated that the intensity pattern is governed by the presence of Cooper-minima, i.e., by a sign change of the radial part of the transition moment function at low electron energies. Since this sign change occurs in the d-continuum the associated odd ΔN transitions are rather small, and even ΔN transitions dominate the experimental spectrum.

In addition to the information on the ion and on the photoionization dynamics, information on the geometry and the electronic character of the exited electronic states of the neutral radical has been obtained from the experiment.

4.4.5. ND_4

One of the most intriguing ZEKE experiments in the last couple of years has been the study of the ND_4 radical [97]. The ammonium radical, NH_4, is of long standing interest to theoreticians and experimentalists alike, since it is a Rydberg-molecule, consisting of a NH_4^+ core and a distant 3s Rydberg electron. The $^2A_1$ electronic ground state is unstable with respect to dissociation into $NH_3 + H$ with vibrational state lifetimes of less than 1 μs. The deuterated ammonium radical, ND_4, on the other hand has a lifetime of more than 10 μs, making it more accessible to the experimentalist. The ND_4 radical was generated from ammonia-clusters that were photodissociated at 202.3 nm according to

$$(ND_3)_2 \rightarrow ND_4 + ND_2$$

Due to the low ionization energy of 37490.7 cm^{-1} the radical could subsequently be ionized by a single photon from a frequency-doubled dye laser. A part of the spectrum of the $ND_4^+X^{+1}A_1 \leftarrow ND_4X\,3s\,^2A_1$ transition is given in the upper trace of Fig. 10, with a

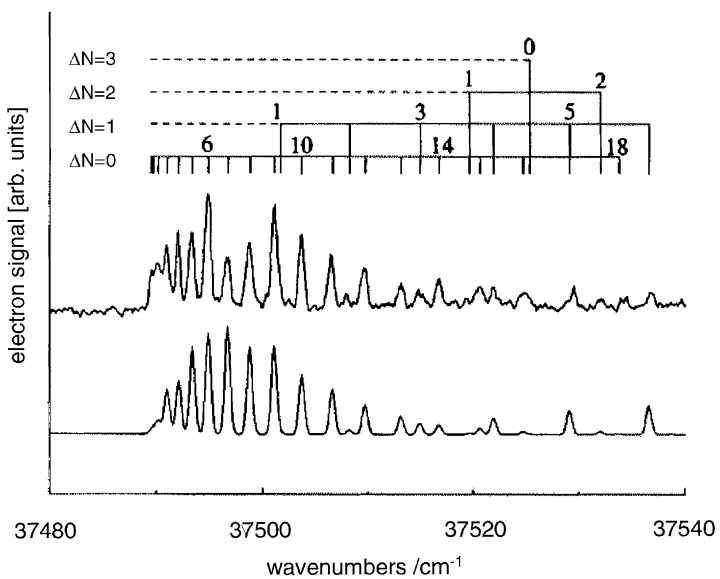

Fig. 10. Part of the rotationally resolved ZEKE-spectrum of ND_4, with a simulation based on the rotational constants of $B_0 = 2.8560$ and $B_0^+ = 2.9855\,cm^{-1}$ given for comparison. Transitions associated with a decrease in rotational angular momentum ΔN appear to the red of the spectrum shown here (reproduced with permission from [97]).

simulation in the lower trace for comparison. Note that $-\Delta N$ transitions appear to the red of the spectrum shown in the figure. A fascinating aspect of this investigation was the determination of the structure of the neutral ground state of ND_4 in addition to the structure of the cation from an analysis of the rotationally resolved band. Rotational constants of $B_0 = 2.8560$ and $B_0{}^+ = 2.9855\,cm^{-1}$ were obtained. From these values N–D bond lengths of $r_0 = 1.0483$ and $r_0{}^+ = 1.0253\,Å$ were deduced for the neutral and the ionic ground state, under the reasonable assumption of tetrahedral symmetry in both states.

Signorell et al. [97] also recorded MATI spectra of ND4 for comparison. Resolution and signal to noise ratio were, however, inferior to the ZEKE-spectra.

4.5. Organic radicals

Studies on organic radicals are often motivated by their importance in combustion reactions. However, investigations pose considerable challenges to the experimentalist. First of all the generation process has to be carried out more carefully, because more side products are possible. Many organic radicals do not possess long-lived excited electronic states, rendering resonant excitation difficult, if not impossible. For a discussion of electronically excited states of radicals, see [50,98]. If one ionizes the radical directly from the ground-state by either one-photon or non-resonant two-photon excitation, care has to be taken that the radicals are vibrationally cold since the large number of vibrational modes can easily lead to spectral congestion even at high-resolution. Nevertheless a number of important organic radicals have been studied by ZEKE-spectroscopy over the last couple of years.

4.5.1. Methyl, CH_3

The methyl radical appears in hydrocarbon combustion and is also believed to be an important intermediate in the growth of diamond thin films by chemical vapor deposition. It was the first polyatomic radical to be studied by ZEKE-spectroscopy with rotational resolution [99]. It was produced by flash pyrolysis of azomethane, CH_3NNCH_3 in Ar at around 1300 K. ZEKE-spectra were recorded using tunable VUV radiation around 126 nm produced by resonant difference-frequency mixing in Kr via the $5p_{5/2} \leftarrow 4p$ two-photon transition at 2×216.67 nm. Fig. 11 shows the experimental spectrum in the upper trace. The lower trace shows a spectrum obtained from ab initio calculations [77] assuming a rotational temperature of 250 K. As visible the agreement between theory and experiment is excellent. Like the $^2A_2''$ ground state of the neutral, the $X^+{}^2A_1'$ of the cation is planar and can be described as an oblate rotor. The various branches are labeled with respect to the $\Delta N = N^+ - N''$ quantum number. The spectrum is dominated by parallel transitions with $\Delta K = K^+ - K'' = 0$, each of the ΔN lines consisting of many closely spaced ΔK subband lines. The computations [77] confirm the dominance of $\Delta K = 0$ transitions and computed the $\Delta K = \pm 2$

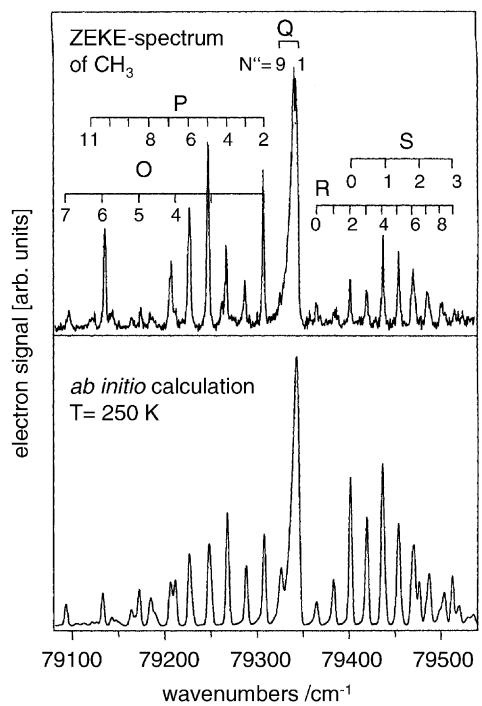

Fig. 11. Rotationally resolved one-photon ZEKE-spectrum of methyl, CH_3. The lower trace shows a simulation based on ab initio calculations. Each of the ΔN transitions assigned in the spectrum consists of closely spaced $\Delta K = 0$ subbands (reproduced with permission from [77]).

subbands to be less than 10% in intensity. Therefore, they are not labeled in the spectrum. There is some disagreement on the low energy side of the spectrum, at some of the P- and O-branch transitions with $\Delta N = -1, -2$ in the computed spectrum. In methyl, like in diatomics, transitions with negative ΔN gather intensity due to rotational autoionization of Rydberg states converging onto rotationally excited states of the ion as described above.

4.5.2. CD_3

The CD_3 radical deserves attention, because it is one of the few radicals studied by the MATI technique so far [100], a variant of ZEKE where the ions instead of the electrons are detected after field ionization of the Rydberg states.

The radical was produced by photodissociation of CD_3I in the ionization region and subsequently excited to the ionization threshold using a $[2 + 1']$ scheme. Since CD_3 is formed with a lot of translational energy a rather complicated arrangement of extraction grids was used to detect the field ionized ions. Despite all efforts a spectrum could only be recorded via the Q-branch of the intermediate $3p_z$ state. The signal was too small to select any isolated rotational level. The case of CD_3 shows, on the other hand, that an investigation of organic radicals by MATI is possible, thus utilizing the additional mass information.

4.5.3. Complexes of alkyl radicals with metal atoms

ZEKE-spectra have also been reported for complexes of the methyl radical with a number of metal atoms, $M\cdots CH_3$, M being Mg, Zn [101] or Cd [102]. The spectra were used to construct molecular orbital (MO) diagrams from the experimental data. The possibility to correlate MO with bands in photoelectron-spectra was one of the driving forces behind the development of PES in the 1960s. For metal-containing compounds with their high density of electronic states this correlation requires a resolution that can only now be achieved. The complexes were produced by laser vaporization of the bare metal in the presence of either CH_3CN or $Sn(CH_3)_4$, both entrained with the carrier gas. In addition to the methyl complexes also the zinc monoethyl complex, ZnC_2H_5, has been studied by ZEKE [103]. Based on an MO model derived from the data, the authors predict a decrease of the relative bond strengths of metal–carbon bonds with an increase in the size of the alkyl radical.

4.5.4. Benzyl, $C_6H_5CH_2$

The benzyl radical was the first organic radical to be investigated by ZEKE-spectroscopy [104–106]. It was generated by photolysis of toluene at 193 nm. Benzyl is one of the few radicals that have long-lived excited states, studied before by laser-induced fluorescence. Therefore, the experiments could be carried out as $[1 + 1']$ experiments through various intermediate vibronic states, yielding an ionization energy of 58,468 cm^{-1}, as well as frequencies of several modes of the $X^{+1}A_1$ cationic ground state. Of particular interest in benzyl is the vibronic coupling between the A^2A_2 and B^2B_2 intermediate states, mediated by modes of b_1 symmetry. Since the intermediate state wave function cannot be separated into an electronic and a vibrational part, non-totally symmetric modes can appear in the ZEKE-spectrum. In a simple picture the mixed vibronic character of the intermediate state will be projected onto the cationic ground state, i.e., in addition to modes of a_1 symmetry the appearance of b_1 modes responsible for the intermediate state coupling is expected [107]. In addition to the ring/CCH bending mode ν_{21}, two more modes were identified to couple the intermediate states strongly, the $\nu_{28}b_1$ in-plane ring deformation mode, and the $(\nu_{17}(a_2) + \nu_{36}(b_2))$ combination band of an out-of-plane CCH bending and an out-of-plane wagging of the CH_2-group. The ν_{29} mode on the other hand, corresponding to in-plane rocking motion of the CH_2-group, appeared only weakly in the ZEKE-spectrum and thus seems to be less important for the vibronic coupling mechanism, in contrast to earlier assumptions. The ZEKE-spectra also gave evidence for vibronic coupling between the A^2A_2 and the C^2A_2 states, mediated by the totally symmetric ν_{13} ring deformation vibration.

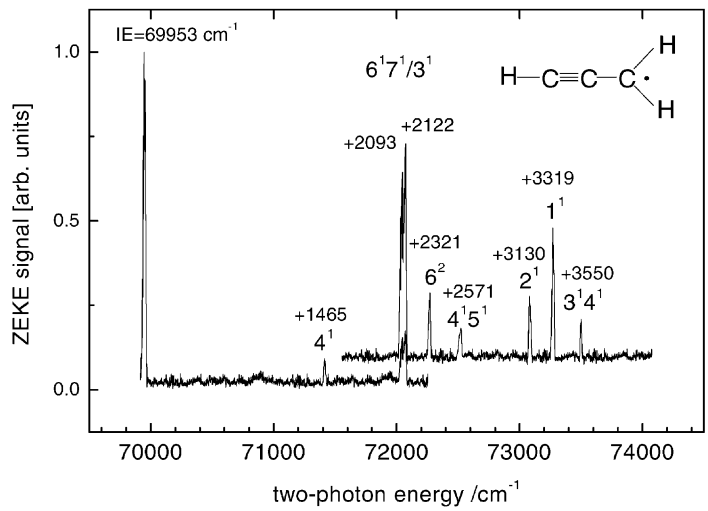

Fig. 12. The ZEKE-spectrum of the propargyl radical, C_3H_3, from 69,900 to 74,200 cm^{-1}. The spectrum is dominated by the origin band, with several bands visible that correspond to vibrationally excited ionic states. Their energy relative to the origin band, as well as the assignments are given in the spectrum (reproduced with permission from [36]).

4.5.5. Propargyl, HC≡C–CH$_2$

The propargyl radical, C_3H_3, is thought to be a central intermediate in the formation of soot. Interest in the structure of the cation also originates from the observation of $C_3H_3^+$ in flames [108] and from the possible role it might play in interstellar chemistry as a precursor to propadienylidene, H_2CCC, through low energy electron attachment [109].

No structured intermediate state permitting resonant excitation is known in the radical. Therefore, the ZEKE spectrum was recorded via non-resonant one-color two-photon ionization [36] using a single frequency-doubled dye laser. The ZEKE spectrum of propargyl from 69,900 to 74,000 cm^{-1} is shown in Fig. 12. The most intense feature is the origin band, centered around 69,950 cm^{-1}, indicating a relatively small geometry change upon ionization. Since an electron is removed from a non-bonding carbon p-orbital upon ionization, this can be readily understood in a qualitative picture. The IE of 69,953 ± 10 cm^{-1}, corresponding to 8.673 eV, is in excellent agreement with an earlier experimental value of 8.67 ± 0.02 eV obtained from conventional photoelectron-spectra [110] as well as with the ab initio value of 8.65 eV [111].

Several transitions into excited vibrational states of the ion appear with significantly lower intensity as compared to the origin band. Some bands, like the acetylenic C–H stretch ν_1 and the C–H_2 stretch ν_2 are readily assigned, while for others the ab initio frequencies obtained from coupled-cluster calculations [111] proved to be helpful. In contrast to the calculations discussed earlier, these calculations do not take the wave function of the free electron into account and thus offer no detailed insight into the ionization dynamics. Only the assignment of the components of the Fermi-resonance doublet around 2100 cm^{-1} is not clear yet. The better agreement with the calculations is obtained upon assigning the higher energy band at 2122 cm^{-1} to the C–C stretch, 3^1, and the lower one to the $6^1 7^1$ combination band. In a recent matrix isolation study, however, the reverse assignment was suggested [112]. Overall the calculated and experimental frequencies match within 1% for the fundamentals and 2% for combination bands and overtones. The ZEKE-spectrum of propargyl can be well understood within the FC picture: only totally symmetric fundamental vibrations appear, and even the relative intensities observed in the

spectrum are comparable to the ones calculated in [111].

4.5.6. Allyl, C_3H_5

Allyl is currently the best understood hydrocarbon radical. High-resolution IR diode-laser spectra of the electronic ground state [57,113] as well as absorption [114,115] and REMPI-spectra [116–118] of electronically excited states are available. Considerable interest was also directed on the dynamics of allyl. The primary photophysical process upon photoexcitation were studied by time-resolved PES [119–121], the photodissociation dynamics and unimolecular fragmentation were investigated by Doppler-spectroscopy [122] and translational energy spectroscopy [49] of the photofragments. Allyl thus serves as the model system for the spectroscopy and dynamics of radicals. Being a C_3 hydrocarbon, its chemistry is also of relevance in combustion processes where allyl is considered to be an intermediate in the formation of soot and polyaromatic hydrocarbons [123].

An earlier photoelectron spectrum yielded the IE of allyl [124], but little structural information was available beyond that. It was therefore reinvestigated by ZEKE-spectroscopy in our group [125]. Allyl can be generated at high number density by flash pyrolysis of 1,5-hexadiene. This precursor cleaves into two allyl units and produces no other side products. An efficient generation of allyl from allyl iodide by photolysis [126] or in an electric discharge [57] was also reported.

The ZEKE-spectra were recorded through various vibronic levels of the resonant intermediate B^2A_1, C^2B_1 and D^2B_2 states. This is remarkable because the lifetimes of these states were measured to be on the order of 20 ps and less [120]. Two ZEKE-spectra are shown as representative examples in Fig. 13; the upper trace shows the spectrum recorded in a $[1 + 1']$ through the C $0_0{}^0$ band, in the lower trace the $[2 + 1']$ spectrum recorded through the B $0_0{}^0$ state is depicted. The $[1 + 1']$ spectrum is remarkably simple and dominated by a single transition into the ionic origin band. Since the experimentally determined geometry of the C-state [117] is very similar to the calculated geometry of the ionic ground state [125,127], such a simple

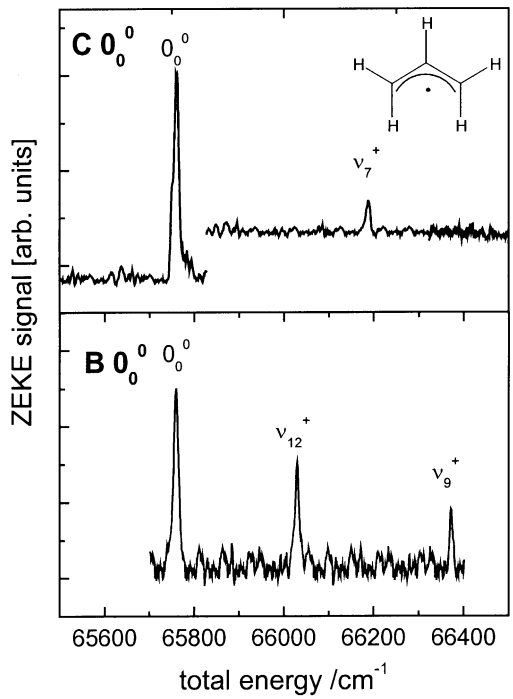

Fig. 13. The ZEKE-spectrum of allyl, C_3H_5, recorded by $[1 + 1']$ excitation through the C-state origin (upper trace) is dominated by a single transition to the ionic origin and shows little vibrational activity. In contrast, the spectrum obtained by $[2 + 1']$ excitation through the B-state origin (lower trace) shows considerable activity in low-frequency modes, indicating a change in geometry upon ionization.

spectrum is expected from FC considerations. Only the fundamental of the C–C–C bending vibration $\nu_7{}^+$ appears weakly in addition because of a slight decrease in the CCC angle upon ionization. This picture was confirmed by several other spectra recorded through various other intermediate vibronic bands.

The spectrum recorded through the B-state origin, on the other hand, shows considerable activity in low-frequency modes. With the aid of ab initio calculations the two bands were assigned to the $\nu_9{}^+$ and $\nu_{12}{}^+$ fundamentals of a_2 and b_1 symmetry, respectively. The two modes correspond to conrotatory and disrotatory motion of the $–CH_2$ groups out of the molecular plane. Their appearance thus indicates a geometry change along both coordinates upon ionization. Interestingly, an earlier REMPI study already

suggested a non-planar geometry of the B 0_0^0 state from a rotational band contour analysis [117,128]. The ZEKE-spectrum thus confirms the non-planar geometry of the B state origin and provides another example for the possibility to deduce information on the neutral radical from high-resolution spectra of the ion. The double minimum potential along the ν_9 and ν_{12} modes appears as a consequence of strong vibronic coupling between the close-lying B, C and D states (pseudo-Jahn–Teller interaction) [129].

4.5.7. CH_3S

The only organic radical containing a heteroatom that has been investigated by ZEKE-spectroscopy so far is the sulfur-containing compound CH_3S. Its $X^{+3}A_2 \leftarrow X^2E_{1/2,3/2}$ transition into the ionic ground state was investigated using non-resonant two-photon excitation [130]. The radical was produced photolytically from either the thiol CH_3SH or the disulfide H_3CSSCH_3 in the ionization region, thus the radical was internally hot. Rotational temperatures of 250 K (thiol-precursor) and 800–900 K (disulfide-precursor) were estimated for the radical. Also both spin–orbit components of the electronic ground state were populated, with relative intensities depending on the precursor employed. Despite these difficulties, reasonable rotational constants have been obtained for the ionic ground state from a fit of the rotational band contours.

4.5.8. Measurements of appearance energies of radicals by ZEKE-spectroscopy

As depicted in Fig. 1 the determination of accurate bond dissociation energies requires not only accurate IEs, but also an equally high accuracy in the determination of appearance energies (AE). Recently such accurate AEs have been obtained for CH_3^+ and C_2H^+ from PFI measurements of CH_4 and C_2H_2, respectively [4]. In these measurements, carried out at a synchrotron beamline of the Advanced Light Source in Berkeley, the breakdown curves for CH_4/CH_3^+ and C_2H_2/C_2H^+ coincided with step-like features in the ZEKE-spectra of the parent molecules at energies of 14.323 (CH_4) and 17.3576 eV (C_2H_2), permitting to extract accurate 0 K AEs. Although these are ZEKE-spectra of stable molecules rather than radicals, the experiments were driven by one of the motivations behind the high-resolution PES of radicals, namely the determination of accurate bond dissociation energies, and thus deserve to be mentioned here. In the future we will probably see experiments where both of the properties shown in Fig. 1 that are necessary to evaluate bond energies are measured by ZEKE-spectroscopy or other methods based on PFI.

4.5.9. ZEKE-spectroscopy and the Franck–Condon principle

As mentioned above several ZEKE-spectra cannot be analyzed within a simple FC picture. Transitions into formally symmetry forbidden non-totally symmetric vibrations of the cation are often observed [131–133], and sometimes, e.g., for Ag_2, even a complete breakdown of the FC picture occurs [72,73]. On the other hand, the spectra of many radicals discussed in the preceding sections are readily understood within the FC-framework. In the ZEKE-spectrum of propargyl no symmetry forbidden vibrations show up, and the measured intensities are well represented by simple calculations that do not even take the electron wave function into account [111]. In allyl and benzyl on the other hand the appearance of non-totally symmetric modes can be explained by vibronic coupling in electronically excited states of the neutral, i.e., in the initial state.

Several possible reasons for anomalous relative vibronic band intensities, among them the presence of Cooper-minima and shape resonances, and interactions between Rydberg series were summarized recently [134]. Deviations from the FC pictures have also been observed in conventional PES and were attributed to the interaction of forbidden states with allowed continua [135]. Most experiments are performed on stable closed-shell molecules that yield open-shell cations upon ionization, with relatively low-lying excited states. Just like in the case of rotation, low-*n* Rydberg states converging onto excited electronic states of the cation might thus be able to couple to the continuum of high-*n* states converging

to the electronic ground state. Such a mechanism, namely spin–orbit autoionization, was invoked to explain the unexpected intensity of the two $^2E_{1/2}$ and $^2E_{3/2}$ spin–orbit states in the ZEKE-spectra of CO_2 [136]. Rydberg states converging onto excited electronic states of the cation might also couple to high-*n* Rydberg states converging to a formally forbidden vibrational mode of the cationic ground state, giving it spectral intensity this way. The argument is probably equivalent to the suggestion of Cockett et al. to treat the occurrence of formally forbidden vibrations as a vibronic coupling problem and to use the full wave function of the cation in a discussion of vibronic selection rules instead of separating them into an electronic and a vibrational part [133]. This seems to be appropriate because in naphthalene, for example, the D_1 state is less than 1 eV above the D_0 state [133].

The photoionization of radicals, on the other hand, leads to the formation of closed-shell cations, with the next excited state being several eV away in energy. In allyl, for example, the first excited state of the ion is about 5 eV above the IE [137]. The density of Rydberg states converging onto the excited ionic state is negligible in the region of the ionization threshold, rendering vibronic interactions much less likely than in stable molecules. Of course other possibilities for intensity perturbations in radicals still remain. Unusual vibrational intensities were observed in the ZEKE-spectra of NO_2 and assigned to couplings between Rydberg states converging onto different rotational and vibrational states of the cation [81–83,134]. Although it remains to be confirmed in the future, it is nevertheless possible that the ZEKE-spectra of radicals are more likely to be amenable to a simple FC-analysis than the spectra of stable molecules.

4.5.10. Outlook

There is still a large number of interesting radicals that just wait to be studied by ZEKE-spectroscopy. Among them are systems like ethyl or vinyl that are expected to have a non-classical cationic structure. In the case of vinyl information on the non-classical structure was already extracted from conventional photoelectron-spectra [138]. The superior resolution of ZEKE-spectroscopy permits to explore the potential energy surface in more detail and allows for a much better theoretical description of these species. Another interesting class are small carbenes, that play an important role in astrochemistry [139], but are also popular as model compounds for theory [140]. And there is of course a large number of radicals containing O, N or Si atoms that are important in all kinds of reactive environments. It is hoped that the present review serves as a starting point for people who reach out for investigations of so far unexplored radicals, using ZEKE or other methods based on PFI.

5. Summary

New techniques based on the PFI of Rydberg states, like ZEKE-spectroscopy, permit to record photoelectron-spectra at an unprecedented resolution. The technique has matured over the last 15 years and now allows to choose the systems to be studied by their chemical relevance. Radicals are such a class of interesting molecules because of their role in the chemistry of reactive environments, like combustion engines, chemical vapor deposition or interstellar space. The size of the systems studied by ZEKE-spectroscopy ranges from diatomics to medium sized organic radicals like allyl or benzyl. Beside accurate IEs and structural information on the cation, information on the neutral radical can be obtained from the spectra.

Acknowledgements

I would like to thank Klaus Müller-Dethlefs (York, UK) for many insightful discussions on ZEKE-spectroscopy over the last 12 years, and Peter Chen (ETH Zürich) for introducing me to the wonderful world of organic radicals.

References

[1] J.H.D. Eland, Photoelectron-spectroscopy, Butterworth, London, 1974.

[2] K. Kimura, S. Katsumata, Y. Achiba, T. Yamazaki, S. Iwata, Handbook of He I Photoelectron-Spectra of Fundamental Organic Molecules, Japan Scientific Society, Tokyo, 1981.
[3] J.A. Blush, H. Clauberg, D.W. Kohn, D.W. Minsek, X. Zhang, P. Chen, Acc. Chem. Res. 25 (1992) 385.
[4] K.M. Weitzel, G.K. Jarvis, M. Malow, T. Baer, Y. Song, C.Y. Ng, Phys. Rev. Lett. 86 (2001) 3526.
[5] J. Baker, M. Barnes, M.C.R. Cockett, J.M. Dyke, A.M. Ellis, M. Feher, E.P.F. Lee, A. Morris, H. Zamanpour, J. Electron Spectrosc. 51 (1990) 487.
[6] P. Chen, in: C.Y. Ng, T. Baer, I. Powis (Eds.), Unimolecular and Bimolecular Reaction Dynamics, Wiley, New York, 1994, p. 371.
[7] K. Müller-Dethlefs, M. Sander, E.W. Schlag, Z. Naturforsch. 39a (1984) 1089.
[8] K. Müller-Dethlefs, E.W. Schlag, Ann. Rev. Phys. Chem. 42 (1991) 109.
[9] K. Müller-Dethlefs, O. Dopfer, T.G. Wright, Chem. Rev. 94 (1994) 1845.
[10] K. Müller-Dethlefs, E.W. Schlag, Angew. Chem. Int. Ed. Engl. 37 (1998) 1346.
[11] E.W. Schlag, R.D. Levine, Comments At. Mol. Phys. 33 (1997) 159.
[12] A. Held, E.W. Schlag, Acc. Chem. Res. 31 (1998) 467.
[13] E.W. Schlag, ZEKE-Spectroscopy, Cambridge University Press, Cambridge, 1998.
[14] D.-S. Yang, P.A. Hackett, J. Electron Spectrosc. 106 (2000) 153.
[15] U. Boesl, C. Bäßmann, E.W. Schlag, in: C.Y. Ng (Ed.), Photoionization and Photodetachment, World Scientific, Singapore, 1999.
[16] U. Boesl, W.J. Knott, Mass Spectrom. Rev. 17 (1998) 275.
[17] A. Held, L.Y. Baranov, H.L. Selzle, E.W. Schlag, J. Chem. Phys. (1997) 6848.
[18] F. Merkt, Ann. Rev. Phys. Chem. 48 (1997) 675.
[19] E.W. Schlag, W.B. Peatman, K. Müller-Dethlefs, J. Electron Spectrosc. 66 (1993) 1.
[20] T. Baer, P.-M. Guyon, in: C.Y. Ng, T. Baer, I. Powis (Eds.), High-Resolution Laser Photoionization and Photoelectron Studies, Wiley, New York, 1995.
[21] G. Reiser, W. Habenicht, K. Müller-Dethlefs, E.W. Schlag, Chem. Phys. Lett. 152 (1988) 119.
[22] W.A. Chupka, J. Chem. Phys. 98 (1993) 4520.
[23] W.A. Chupka, J. Chem. Phys. 99 (1993) 5800.
[24] M.J.J. Vrakking, J. Chem. Phys. 105 (1996) 7336.
[25] F. Remacle, R.D. Levine, E.W. Schlag, H.L. Selzle, A. Held, J. Phys. Chem. 100 (1996) 15320.
[26] F. Merkt, J. Chem. Phys. 100 (1994) 2623.
[27] M.J.J. Vrakking, I. Fischer, D.M. Villeneuve, A. Stolow, J. Chem. Phys. 103 (1995) 4538.
[28] H. Palm, R. Signorell, F. Merkt, Phil. Trans. R. Soc. London Ser. A 355 (1997) 1551.
[29] M.J.J. Vrakking, Phil. Trans. R. Soc. London Ser. A 355 (1997) 1693.
[30] R. Lindner, H.-J. Dietrich, K. Müller-Dethlefs, Chem. Phys. Lett. 228 (1994) 4.
[31] H.J. Dietrich, K. Müller-Dethlefs, L.Y. Baranov, Phys. Rev. Lett. 76 (1996) 3530.
[32] F. Merkt, H. Schmutz, J. Chem. Phys. 108 (1998) 10033.
[33] A. Osterwalder, F. Merkt, Phys. Rev. Lett. 82 (1999) 1831.
[34] P.C. Engelking, Chem. Rev. 91 (1991) 399.
[35] M. Takahashi, H. Ozeki, K. Kimura, Chem. Phys. Lett. 181 (1991) 255.
[36] T. Gilbert, R. Pfab, I. Fischer, P. Chen, J. Chem. Phys. 112 (2000) 2575.
[37] P. Kruit, F.H. Read, J. Phys. E: Sci. Instrum. 16 (1983) 313.
[38] G.I. Nemeth, H.L. Selzle, E.W. Schlag, Chem. Phys. Lett. 215 (1993) 151.
[39] D. Bahatt, O. Cheshnovsky, U. Even, Z. Phys. Chem. 184 (1994) 253.
[40] J.B. Milan, W.J. Buma, C.A. de Lange, J. Chem. Phys. 104 (1996) 521.
[41] L. Zhu, P.M. Johnson, J. Chem. Phys. 94 (1991).
[42] P.M. Johnson, L. Zhu, Int. J. Mass Spectrom. Ion Proc. 131 (1994) 193.
[43] H. Krause, H.-J. Neusser, J. Chem. Phys. 97 (1992) 5923.
[44] H.-J. Dietrich, R. Lindner, K. Müller-Dethlefs, J. Chem. Phys. 101 (1994) 3399.
[45] P. Chen, S.D. Colson, W.A. Chupka, J.A. Berson, J. Phys. Chem. 90 (1986) 2319.
[46] D.W. Kohn, H. Clauberg, P. Chen, Rev. Sci. Instrum. 63 (1992) 4003.
[47] P. Chen, in: U.H. Brinker (Ed.), Advances in Carbene Chemistry, JAI Press, New York, 1998.
[48] N. Hansen, H. Mäder, F. Temps, Chem. Phys. Lett. 327 (2000) 97.
[49] D. Stranges, M. Stemmler, X. Yang, J.D. Chesko, A.G. Suits, Y.T. Lee, J. Chem. Phys. 109 (1998) 5372.
[50] X.Q. Tan, T.G. Wright, T.A. Miller, in: J.M. Hollas, D. Phillips (Eds.), Jet Spectroscopy Molecular Dynamics, Blackie Academic and Professional, London, 1995.
[51] C.C. Carter, J.R. Atwell, S. Gopalakrishnan, T.A. Miller, J. Phys. Chem. 104 (2000) 9165.
[52] A.T. Droege, P.C. Engelking, Chem. Phys. Lett. 96 (1983) 316.
[53] R. Schlachta, G.M. Lask, S.H. Tsay, V.E. Bondybey, Chem. Phys. 155 (1991) 267.
[54] A. Thoma, B.E. Wurfel, R. Schlachta, G.M. Lask, V.E. Bondybey, J. Phys. Chem. 96 (1992) 7231.
[55] K.N. Rosser, Q.-Y. Wang, C.M. Western, J. Chem. Soc., Faraday Trans. 89 (1993) 391.
[56] D.T. Anderson, S. Davis, T.S. Zwier, D.J. Nesbitt, Chem. Phys. Lett. 258 (1996) 207.
[57] D. Uy, S. Davis, D.J. Nesbitt, J. Chem. Phys. 109 (1998) 7793.
[58] S. Davis, D. Uy, D.J. Nesbitt, J. Chem. Phys. 112 (2000) 1823.
[59] V.E. Bondybey, J.H. English, J. Chem. Phys. 74 (1981) 6978.
[60] T.G. Dietz, M.A. Duncan, D.E. Powers, R.E. Smalley, J. Chem. Phys. 74 (1981) 6511.
[61] H.H. Fielding, T.P. Softley, F. Merkt, Chem. Phys. 155 (1991) 257.

[62] J.W. Hepburn, in: A. Myers, T.R. Rizzo (Eds.), Laser Techniques in Chemistry, Wiley, New York, 1994.
[63] E. Waterstradt, R. Jung, H.-J. Dietrich, K. Müller-Dethlefs, Rev. Sci. Instrum. 64 (1993) 3104.
[64] G.K. Jarvis, K.-M. Weitzel, M. Malow, T. Baer, Y. Song, C.Y. Ng, Rev. Sci. Instrum. 70 (2000) 3892.
[65] I. Fischer, A. Strobel, J. Staecker, G. Niedner-Schatteburg, K. Müller-Dethlefs, V.E. Bondybey, J. Chem. Phys. 96 (1992) 7171.
[66] A. Strobel, I. Fischer, A. Lochschmidt, K. Müller-Dethlefs, V.E. Bondybey, J. Phys. Chem. 98 (1994) 2024.
[67] J. Xie, R.N. Zare, J. Chem. Phys. 93 (1990) 3033.
[68] A.D. Buckingham, B.J. Orr, M.J. Sichel, Phil. Trans. R. Soc. London Ser. A 268 (1970) 147.
[69] I. Fischer, R. Lindner, K. Müller-Dethlefs, J. Chem. Soc., Faraday Trans. 90 (1994) 2425.
[70] R. Signorell, F. Merkt, Mol. Phys. 92 (1997) 793.
[71] W.A. Chupka, E. Grant, J. Phys. Chem. 103 (1999) 6127.
[72] G.I. Nemeth, H. Ungar, C. Yeretzian, H.L. Selzle, E.W. Schlag, Chem. Phys. Lett. 228 (1994) 1.
[73] C. Yeretzian, R.H. Hermann, H. Ungar, H.L. Selzle, E.W. Schlag, S.H. Lin, Chem. Phys. Lett. 239 (1995) 61.
[74] M.J. Seaton, Rep. Prog. Phys. 46 (1983) 167.
[75] C.H. Greene, C. Jungen, Adv. At. Mol. Phys. 21 (1985) 51.
[76] K. Wang, J.A. Stephens, V. McKoy, J. Phys. Chem. 97 (1993) 9874.
[77] K. Wang, V. McKoy, Ann. Rev. Phys. Chem. 46 (1995) 275.
[78] H.P. Loock, B. Simard, S. Wallin, C. Linton, J. Chem. Phys. 109 (1998) 8980.
[79] G. Reiser, K. Müller-Dethlefs, J. Phys. Chem. 96 (1992) 9.
[80] A. Strobel, I. Fischer, J. Staecker, G. Niedner-Schatteburg, K. Müller-Dethlefs, V.E. Bondybey, J. Chem. Phys. 97 (1992) 2332.
[81] G. Bryant, Y. Jiang, E.R. Grant, Chem. Phys. Lett. 200 (1992) 495.
[82] G. Bryant, Y. Jiang, M. Martin, E. Grant, J. Phys. Chem. 96 (1992) 6875.
[83] G.P. Bryant, Y.N. Jiang, M. Martin, E.R. Grant, J. Chem. Phys. 101 (1994) 7199.
[84] R.T. Wiedmann, R.G. Tonkyn, M.G. White, K. Wang, V. McKoy, J. Chem. Phys. 97 (1992) 768.
[85] E. de Beer, C.A. de Lange, J.A. Stephens, K. Wang, V. McKoy, J. Chem. Phys. 95 (1991) 714.
[86] C.A. de Lange, Adv. Chem. Phys. 117 (2001) 1.
[87] C.-W. Hsu, D.P. Baldwin, C.-L. Liao, C.Y. Ng, J. Chem. Phys. 100 (1994) 8047.
[88] F. Merkt, T.P. Softley, Int. Rev. Phys. Chem. 12 (1993) 205.
[89] F. Merkt, T.P. Softley, in: I. Powis, T. Baer, C.-Y. Ng (Eds.), High-Resolution Laser Photoionization and Photoelectron Studies, Wiley, Chichester, 1995, p. 119.
[90] A.M. Rijs, E.H.G. Backus, C.A. de Lange, N.P.C. Westwood, M.H.M. Janssen, J. Electron Spectrosc. 112 (2000) 151.
[91] J.B. Milan, W.J. Buma, C.A. de Lange, K. Wang, V. McKoy, J. Chem. Phys. 107 (1997) 2782.
[92] J.B. Milan, W.J. Buma, C.A. de Lange, K. Wang, V. McKoy, J. Chem. Phys. 103 (1995) 3262.
[93] E. de Beer, M. Born, C.A. de Lange, N.P.C. Westwood, Chem. Phys. Lett. 186 (1991) 40.
[94] K. Wang, J.A. Stephens, V. McKoy, E. de Beer, C.A. de Lange, N.P.C. Westwood, J. Chem. Phys. 97 (1992) 211.
[95] D.H.A. ter Steege, M. Smits, C.A. de Lange, N.P.C. Westwood, J.B. Peel, L. Visscher, Faraday Discuss. 115 (2000) 259.
[96] K. Wang, J.A. Stephens, V. McKoy, J. Phys. Chem. 98 (1994) 460.
[97] R. Signorell, H. Palm, F. Merkt, J. Chem. Phys. 106 (1997) 6523.
[98] M.N.R. Ashfold, S.G. Clement, J.D. Howe, C.M. Western, J. Chem. Soc., Faraday Trans. 89 (1993) 1153.
[99] J.A. Blush, P. Chen, R.T. Wiedmann, M.G. White, J. Chem. Phys. 98 (1993) 3557.
[100] H. Dickinson, T. Chelmick, T.P. Softley, Chem. Phys. Lett. 338 (2001) 37.
[101] T.A. Barckholtz, D.E. Powers, T.A. Miller, B.E. Bursten, J. Am. Chem. Soc. 121 (1999) 2576.
[102] S.I. Panov, D.E. Powers, T.A. Miller, J. Chem. Phys. 108 (1998) 1335.
[103] M.B. Pushkarsky, V.L. Stakhursky, T.A. Miller, J. Phys. Chem. A 104 (2000) 9184.
[104] G.C. Eiden, F. Weinhold, J.C. Weisshaar, J. Chem. Phys. 95 (1991) 8665.
[105] G.C. Eiden, J.C. Weisshaar, J. Phys. Chem. 95 (1991) 6194.
[106] G.C. Eiden, K.T. Lu, J. Badenhoop, F. Weinhold, J.C. Weisshaar, J. Chem. Phys. 104 (1996) 8886.
[107] G.C. Eiden, J.C. Weisshaar, J. Chem. Phys. 104 (1996) 8896.
[108] J.L. Goodings, D.K. Bohme, C.-W. Ng, Combust. Flame 36 (1979) 27.
[109] J.M. Vrtilek, C.A. Gottlieb, E.W. Gottlieb, T.C. Killian, P. Thaddeus, Astrophys. J. 346 (1990) L53.
[110] D.W. Minsek, P. Chen, J. Phys. Chem. 94 (1990) 8399.
[111] P. Botschwina, R. Oswald, J. Fluegge, M. Horn, Z. Phys. Chem. (Munich) 188 (1995) 29.
[112] M. Wyss, E. Riaplov, J.P. Maier, J. Chem. Phys. 114 (2001) 10355.
[113] E. Hirota, C. Yamada, M. Okunishi, J. Chem. Phys. 97 (1992) 2963.
[114] A.B. Callear, H.K. Lee, Trans. Faraday Soc. 64 (1968) 308.
[115] K. Tonokura, M. Koshi, J. Phys. Chem. 104 (2000) 8456.
[116] J.W. Hudgens, C.S. Dulcey, J. Phys. Chem. 89 (1985) 1505.
[117] J.A. Blush, D.W. Minsek, P. Chen, J. Phys. Chem. 96 (1992) 10150.
[118] D.W. Minsek, J.A. Blush, P. Chen, J. Phys. Chem. 96 (1992) 2025.
[119] T. Schultz, I. Fischer, J. Chem. Phys. 107 (1997) 8197.
[120] T. Schultz, I. Fischer, J. Chem. Phys. 109 (1998) 5812.
[121] T. Schultz, J.S. Clarke, H.-J. Deyerl, T. Gilbert, I. Fischer, Faraday Discuss. 115 (2000) 17.
[122] H.-J. Deyerl, I. Fischer, P. Chen, J. Chem. Phys. 110 (1999) 1450.
[123] J.A. Miller, R.J. Kee, C.K. Westbrook, Ann. Rev. Phys. Chem. 41 (1990) 345.
[124] F.A. Houle, J.L. Beauchamp, J. Am. Chem. Soc. 100 (1978) 3290.
[125] T. Gilbert, I. Fischer, P. Chen, J. Chem. Phys. 113 (2000) 561.

[126] J.D. Getty, M.J. Burmeister, S.G. Westre, P.B. Kelly, J. Am. Chem. Soc. 113 (1991) 801.
[127] B. Reindl, T. Clark, P.V.R. Schleyer, J. Comp. Chem. 18 (1997) 533.
[128] D.W. Minsek, P. Chen, J. Phys. Chem. 97 (1993) 13375.
[129] G. Fischer: Vibronic Coupling, Academic Press, London, 1984.
[130] C.-W. Hsu, C.Y. Ng, J. Chem. Phys. 101 (1994) 5596.
[131] G. Reiser, D. Rieger, T.G. Wright, K. Müller-Dethlefs, E.W. Schlag, J. Phys. Chem. 97 (1993) 4335.
[132] I. Fischer, A. Lochschmidt, A. Strobel, G. Niedner-Schatteburg, K. Müller-Dethlefs, V.E. Bondybey, Chem. Phys. Lett. 202 (1993) 542.
[133] M.C.R. Cockett, H. Ozeki, K. Okuyama, K. Kimura, J. Chem. Phys. 98 (1993) 7763.
[134] W.A. Chupka, E.R. Grant, J. Phys. Chem. A 103 (1999) 6127.
[135] W.A. Chupka, J. Chem. Phys. 87 (1987) 1488.
[136] F. Merkt, S.R. Mackenzie, R.J. Rednall, T.P. Softley, J. Chem. Phys. 99 (1993) 8430.
[137] T.-K. Ha, H. Baumann, J.F.M. Oth, J. Chem. Phys. 85 (1986) 1438.
[138] J.A. Blush, P. Chen, J. Phys. Chem. 96 (1992) 4138.
[139] P. Thaddeus, C.A. Gottlieb, R. Mollaaghababa, J. Vrtilek, J. Chem. Soc., Faraday Trans. 89 (1993) 2125.
[140] H.F. Bettinger, P.V.R. Schleyer, P.R. Schreiner, H.F. Schaefer III, in: P.V.R. Schleyer (Ed.), Encyclopedia of Computational Chemistry, Wiley, Chichester, 1998, p. 183.
[141] M.C.R. Cockett, K. Müller-Dethlefs, T.G. Wright, Annu. Rep. Prog. Chem. C 94 (1998) 327.